

Article

Optimal Design of Photovoltaic Power Plant Using Hybrid Optimisation: A Case of South Algeria

Tekai Eddine Khalil Zidane ^{1,*}, Mohd Rafi Adzman ^{1,2}, Mohammad Faridun Naim Tajuddin ¹, Samila Mat Zali ¹, Ali Durusu ³ and Saad Mekhilef ^{4,5,6}

¹ School of Electrical Systems Engineering, Universiti Malaysia Perlis, Arau 02600, Malaysia; mohdrafi@unimap.edu.my (M.R.A.); faridun@unimap.edu.my (M.F.N.T.); samila@unimap.edu.my (S.M.Z.)

² Centre of Excellence for Renewable Energy (CERE), School of Electrical Systems Engineering, Universiti Malaysia Perlis, Arau 02600, Malaysia

³ Department of Electrical Engineering, Davutpasa Campus, Yildiz Technical University, Istanbul 34220, Turkey; adurusu@yildiz.edu.tr

⁴ Power Electronics and Renewable Energy Research Laboratory (PEARL), Department of Electrical Engineering, University of Malaya, Kuala Lumpur 50603, Malaysia; saad@um.edu.my

⁵ School of Software and Electrical Engineering, Swinburne University of Technology, Victoria 3122, Australia

⁶ Center of Research Excellence in Renewable Energy and Power Systems, King Abdulaziz University, Jeddah 21589, Saudi Arabia

* Correspondence: zidanetekai@hotmail.fr

Received: 5 March 2020; Accepted: 30 April 2020; Published: 1 June 2020



Abstract: Considering the recent drop (up to 86%) in photovoltaic (PV) module prices from 2010 to 2017, many countries have shown interest in investing in PV plants to meet their energy demand. In this study, a detailed design methodology is presented to achieve high benefits with low installation, maintenance and operation costs of PV plants. This procedure includes in detail the semi-hourly average time meteorological data from the location to maximise the accuracy and detailed characteristics of different PV modules and inverters. The minimum levelised cost of energy (LCOE) and maximum annual energy are the objective functions in this proposed procedure, whereas the design variables are the number of series and parallel PV modules, the number of PV module lines per row, tilt angle and orientation, inter-row space, PV module type, and inverter structure. The design problem was solved using a recent hybrid algorithm, namely, the grey wolf optimiser-sine cosine algorithm. The high performance for LCOE-based design optimisation in economic terms with lower installation, maintenance and operation costs than that resulting from the use of maximum annual energy objective function by 12%. Moreover, sensitivity analysis showed that the PV plant performance can be improved by decreasing the PV module annual reduction coefficient.

Keywords: optimal design; photovoltaic power plants; hybrid optimisation; LCOE; PV module reduction

1. Introduction

Nowadays, solar photovoltaic energy is being utilised in electrical energy generation to meet the quick-growing consumption and the urgent need for power [1]. Grid-connected photovoltaic (PV) systems with a capacity of 3 kW PV modules could meet the electric demand of a 60–90 m² for residential building [2]. By contrast, large-scale PV power plants face some major challenges for the use of vast amounts of components in relation to the cost, reliability, and efficiency, requiring an optimal design of the PV power plant. Recently, the drop in PV module prices of up to 86% from 2010 to

2017 [3] resulted in a decrement in the levelised cost of energy (LCOE) of large-scale PV power plants reaching 0.03 (\$) [4].

TRNSYS software has been used to determine the optimum PV inverter sizing ratios [5]. The simulation has been carried out using three types of inverters with low, medium and high efficiency to determine the maximum total output of the PV system. Furthermore, the PV inverter sizing ratio of the grid-connected has been investigated for eight European locations. Mondol et al. suggested that the installation of a PV system with high-efficiency inverter in the sizing of PV and inverter is more flexible than that of a low-efficiency inverter. Artificial intelligence (AI) methods have also been used to optimise the grid-connected PV power plant, as presented in [6], whereas the PV plant global solution is solved through particle swarm optimisation technique (PSO) and compared with a genetic algorithm (GA), based on the total net economic benefit. However, the PSO algorithm showed better performance than the GA approach used in this study. The optimisation design of the grid-connected PV system is introduced in [7]. The decision variables of the proposed methodology are the type of PV modules, inverter, and tilt angle. The study supports the mathematical models of the PV array, inverter and solar irradiance on tilt PV modules surface. The optimisation process considered three types of inverter, four types of PV modules and seven values of tilt angle, as well as the hourly solar irradiance and ambient temperature. As a result, the optimal design of the system is selected based on maximum efficiency.

In 2012 [8], Sulaiman, S.I., et al. proposed a sizing methodology by using an evolutionary programming sizing algorithm. The optimisation procedure supports all possible combinations of PV modules and inverters considering different types of PV modules and inverters. The technical and economic aspects are included in this method, and both the maximum yield factor and the net present value of the PV system were calculated. Chen et al. have proposed an iterative method for the optimal size of inverter for PV systems with maximum savings in nine locations in the USA [9]. The optimisation procedure has selected the gainful inverter size for each location. Additionally, optimum inverter size lower than or the same as that of PV array rated size can be installed, due to the inverter intrinsic parameters, economic and weather considerations. In 2014, Perez-Gallardo proposed an optimal configuration of the grid-connected PV power plant of different PV technologies by using the GA technique, by considering economic, technical and environmental criteria [10]. This study aims to maximise annual energy generation. Another methodology was proposed in [11] to design a PV plant for the self-consumption mechanism for different capacities in the range of 450–1250 kWp for the university campus. The simulation was performed using PV*SOL software.

A study in [12] investigated the selection and configuration of inverter and PV modules for a PV system for minimising costs. The purchasing costs can be reduced by 16.45% of 10 kW by using this model. However, this evaluation model is applicable only at the lowest price and cannot be applied to achieve the highest efficiency in power production. A mathematical procedure is presented in [13–15] to determine the optimal number of rows and a PV module tilt angle for maximising the profit during PV plant lifetime, by considering the effect of shading on the PV module output power. A work in [16] investigated the design of PV systems grid-connected, considering the PV module degradation rate, to select the optimum inverter size for increased energy and reduced cost. Actual inverters with high efficiency offer a wider range than inverter with low-efficiency for sizing factor to increase the energy generation. Research presented in [17] proposed an eco-design for grid-connected PV systems, on the basis of the combination of multi-objective optimisation and other software. The techno-economic and environmental criteria were optimised simultaneously. The installation of thin-film PV modules in PV systems show an advantage over crystalline silicon ones. A methodology for achieving the optimal configuration of large-scale PV power plants to improve its performance is presented in [18]. The optimisation process was performed using different algorithms and is considered to minimise the LCOE by using crystalline silicon and thin-film cadmium telluride PV module technology. According to this study, the proposed technique of grey wolf optimiser showed improved results compared with the other methods in solving the optimal design of the PV power plant. The PV plant LCOE with the thin film had a lower value than crystalline silicon and is more productive. The work reported in [19] proposed a method to convert the design of PV

power plants to binary linear programming to achieve an economical design. However, in this method, only the number of inverters and PV modules connected in series and parallel were considered as the design variables. Some other methods have also been employed and published by researchers in this topic to propose a suitable configuration and determine the best solution that considers the environment, economic and technical aspects of the PV system [20–36]. Additionally, references [37–41] reviewed the grid-connected PV system optimisation and challenges.

The average time for the input meteorological data is an essential factor in PV system design, because the monthly and daily average time of the meteorological data fails to determine an optimum design, resulting in the oversizing system and high energy losses and increasing the financial risk of the PV plant. Additionally, the geographic latitude of the PV plant installation site can lead to a significant variation of the PV module optimal tilt angle from one location to another, to convert maximum solar irradiance into electricity and make the PV system more profitable [42].

This paper intends to present a methodology for designing PV power plants by considering semi-hourly time-resolution (i.e., 30 min-average) to address the accuracy of the meteorological data variation, and thus determine the PV plant optimal design and increase its performance. The procedure considers the detailed specifications of the different alternatives of PV modules and inverters to determine the optimum component and system topology for the location under study. Three meteorological parameters of solar irradiation, wind speed, and ambient temperature were measured for 1 year at the installation field are considered. Hybrid grey wolf optimiser-sine cosine algorithm (HGWOSCA) [43] and sine cosine algorithm (SCA) [44] were applied as optimisation techniques to solve the PV plant design problem for two different objectives, including minimum levelised cost of energy (LCOE) and maximum annual energy, while considering many design variables for improving the system performance. The contributions of this article to the book of knowledge in this research field are described below.

- The proposed methodology is suitable to be executed using semi-hourly time-resolution (i.e., 30 min-average) values of the meteorological input data in designing the PV power plant and by introducing an actual PV plant field model, by considering the shape and size of the PV power plant installation area, to arrange all the existing components properly.
- The application of a HGWOSCA optimisation approach after the consideration of two objective functions to design the PV power plant was presented.
- A sensitivity study was performed to investigate the effect of the annual PV module reduction coefficient on PV plant performance.
- A review of the Algerian renewable energy target and its integration was presented.

This paper is organised as follows: Section 2 presents an overview of the renewable energy potential of Algeria, and Section 3 presents the work methodology, including the formulation of the design problem, the PV system description and meteorological data and, the proposed design optimization. In Section 4, the HGWOSCA algorithm is described. Section 5 presents the obtained results with the sensitivity study. Finally, Section 6 presents the conclusions of the paper.

2. The Renewable Energy Potential of Algeria

Algeria has an important potential for electricity generation from renewable energy sources, as performed in several recent studies. However, according to reference [45], approximately 0.415% of electricity in Algeria is generated from renewable energy sources in 2014. The diesel generator is the dominant energy source in rural and Saharan regions in Algeria [46].

2.1. Solar Energy

The potential of solar energy in southern Algeria is the largest in all Mediterranean basins, with 1,787,000 km² of Sahara desert, according to the German Aerospace Centre (DLR). The insolation time of almost all the national territory exceeds 2000 h annually and reaches 3900, as shown in

Figure 1 (high plains and Sahara) [47]. Over most of the country and during the day, the energy obtained on a horizontal surface of 1 m² is nearly 5 kWh or about 2263 kWh/m²/year in the south and 1700 kWh/m²/year in the north [48]. This great potential in solar energy compels Algeria to go towards the exploitation of solar energy for power generation, rather than oil and gas. Table 1 shows the rate of sunshine for each region of Algeria.

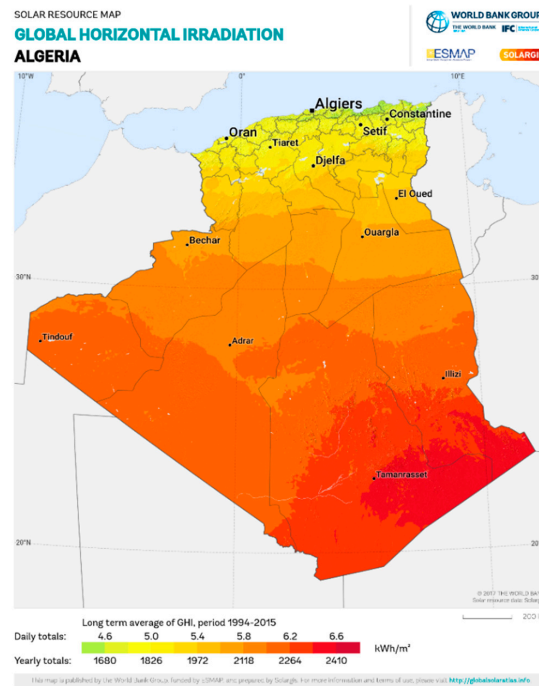


Figure 1. Horizontal Irradiation of Algeria [50].

Table 1. Radiation in Algeria [49].

Region	Coastal	Highlands	Sahara
Area (%)	4	10	86
Average sun hours per year	2650	3000	3500
Energy received kWh/m ² /year	1700	1900	2650

2.2. Other Renewable Energy Potential

Algeria has a considerable average of wind speed that can reach 6 m/s in approximately 50% of the country’s surface. The government plans to promote this energy source. Hydroelectricity potential is modest and has little benefit to the Algerian economy. For geothermal energy, the Renewable Energy Development Centre listed more than 200 hot springs, thereby presenting a favourable outlook to exploit this resource [48]. Finally, the biomass potential in Algeria is considerable. It reaches 5 Mtoe/year, but it is still not consumed. This source of energy offers great promises and should be enhanced [51].

2.3. Algerian Renewable Energy Program

Currently, Algeria focuses on the production of electrical energy from renewable sources, especially on solar energy and grid-connected photovoltaic power plants, for a capacity of several megawatts to reduce its dependence on oil rents, thereby representing approximately 96% of export and 17.36% of GDP in 2014 [52]. It also aims to reduce the use of diesel generators, which is the dominant energy source in rural and Saharan regions in Algeria [46].

The development of green energy sources is a key priority for the Algerian government. Nowadays, enhancing the exploitation of renewable energy is a necessity to decrease the amount of CO₂ emissions, considering that Algeria has shown great interest in signing the historic Paris agreement in 2015 [53]. Furthermore, with such a measure, the government can save conventional resources, which are used to generate electricity. The renewable sources showed a poor share in the total energy compared with the conventional sources [54]. The residential electricity sector reached approximately 42% of the total energy consumption [55]. However, the ambitious national renewable energy program allowed one to reach 27% of renewable energy in the national energy mix [56].

Renewable energy sources are the focus of the 2011–2030 development program adopted by the Algerian government to achieve the installation of 22,000 MW of renewables by 2030, including 10,000 MW for export and 12,000 MW for meeting the national market demand [57]. Notably, photovoltaic energy is the dominant renewable source and is expected to reach a capacity of 13,575 MW, representing 62% of the total power installation, as shown in Table 2. In this ambitious program, the government strategy focuses on the development of photovoltaics on a large scale and prepares for the future of Algeria. The adopted program includes the development of wind and CSP energy, biomass, cogeneration and geothermal sources.

Table 2. Phases of the Algerian renewable energy program [58].

Energy Type	1st Phase 2015–2020 (MW)	2nd Phase 2021–2030 (MW)	Total (MW)
Photovoltaic	3000	10,575	13,575
Wind	1010	4000	5010
CSP	-	2000	2000
Cogeneration	150	250	400
Biomass	360	640	1000
Geothermal	5	10	15
Total	4525	17,475	22,000

2.4. Photovoltaic Power Plants Installed in Algeria

In August 2019, the Algerian company for electricity and gas (Sonelgaz) signed an agreement with five companies to construct nine PV power plants in the southern big Sahara region, with a total capacity of 50 MW [59]. This project aims to make a hybrid energy system with an existing gas turbine and diesel generator. The PV plants are installed in different locations, as shown in the following Table 3:

Table 3. Projects of Photovoltaic power plant installation in Algeria.

N	PV Power Plant	Province	Power (MWp)
1	In Guezzem	Tamanrasset	6
2	Tinzaouatine	Tamanrasset	3
3	Djanet	Illizi	4
4	Bordj Omar Dris	Illizi	3
5	Bordj Badji Mokhtar	Adrar	10
6	Timiaouine	Adrar	2
7	Talmine	Adrar	8
8	Tabelbala	Bechar	3
9	Tindouf	Tindouf	11

Several large-scale PV power plants have been installed and connected to the electric grid in different locations across the country, and most of the PV plants are located in the big Sahara in the South, thereby indicating that Algeria benefits from this source of energy, as shown in Table 4. In addition to the absence of batteries that reduce the total capital cost, this system allows power generation surplus in terms of consumption of the load to be automatically injected into the electric grid.

Table 4. Photovoltaic power plants installed in Algeria.

N	PV Power Plant	Province	Power (MWp)	Energy Production (GWh)-June 2017	Commissining Date	Area (km ²)	Distance to Electric Grid (km)	Voltage Level at Point of Coupling (kV)	PV Modules Type	Topology
1	Adrar	Adrar	20	59.585	Oct-15	0.4	2.8	30	Poly	C
2	Kabertène	Adrar	3	9.584	Oct-15	0.06	0.2	30	Poly	C
3	In Salah	Tamanrasset	5	12.328	Feb-16	0.1	0.5	30	Poly	C
4	Timimoune	Adrar	9	23.822	Feb-16	0.18	9	30	Poly	C
5	Regguen	Adrar	5	12.221	Jan-16	0.1	0.22	30	Poly	C
6	Zaouiat Kounta	Adrar	6	15.213	Jan-16	0.12	0.24	30	Poly	C
7	Aoulef	Adrar	5	12.557	Mar-16	0.1	0.4	30	Poly	C
8	Tamanrasset	Tamanrasset	13	36.41	Nov-15	0.26	8.8	30	Poly	C
9	Djanet	Ilizi	3	10.729	Feb-15	0.06	0.35	30	Poly	C
10	Tindouf	Tindouf	9	6.376	Dec-15	0.18	0.3	30	Poly	C
11	Oued Nechou	Ghardaia	1.1	4.593	Jul-14	0.1	0.4	30	m-Si,c-Si,Thin film, si-amorphe	C
12	Sedret Leghzel	Naâma	20	40.751	May-16	0.42	1.3	60	Poly	C
13	Oued El Kebrit	Souk Ahras	15	28.9	Apr-16	0.32	6.5	30	Poly	C
14	Ain Skhouna	Saida	30	14.213	May-16	0.42	12	60	Poly	C
15	Ain El Bel 1	Djelfa	20	25.134	Apr-16	0.4	3.9	60	Poly	C
16	Ain El Bel 2	Djelfa	33	25.134	Apr-16	0.8	3.9	60	Poly	C
17	Lekhneg 1	Laghouat	20	53.576	Apr-16	0.4	12	60	Poly	C
18	Lekhneg 2	Laghouat	40	53.576	Apr-16	0.8	12	60	Poly	C
19	Telagh	Sidi-Bel-Abbes	12	7.417	Sep-16	0.3	6	60	Poly	C
20	Labiodh Sidi Chikh	El-Bayadh	23	19.146	Nov-18	0.392	0.9	60	Poly	C
21	El Hdjira	Ouargla	30	9.738	Jul-16	0.6	1	60	Poly	C
22	Ain-El-Melh	M'Sila	20	16.473	Sep-17	0.4	0.9	60	Poly	C
23	Oued El Ma	Batna	2	-	Mar-17	0.3	0.5	30	Poly	C

3. Methodology

3.1. Formulation of the Design Problem

The single objective optimisation function is used to find the optimum solution corresponding to the minimum or maximum value defined by the objective function. In contrast, multi-objective optimisation combines two or more individual objective functions to determine a set of trade-off solutions, which allow decision makers to select the most suitable solution based on the problem requirements [60]. In this study, in sizing optimisation methodology depending on the requirements of the power plant designer, each of the two objectives can be used to produce an optimal design for the PV power plant. In addition, for comparison purposes, the optimum values are calculated by using each objective function individually to evaluate the PV power plant performance.

Furthermore, multi-objective optimisation can be used in the design of PV systems with a small capacity in the range of kW, with a small number of PV modules and inverters or in hybrid renewable energy systems for example (PV-wind) or (PV-diesel generator-battery). However, in large scale PV power plants (i.e., >200 kW nominal power rating—the largest plants reaching several tens of MW of capacity), with a considerable number of components required in PV plant installation, it is well-known that the levelised cost of energy (LCOE) is applied to enable the reduction of the PV plant cost per watt of nominal power that is installed [61,62], for this reason, single objective optimisation is used. Additionally, a recent study is presented in [63] to investigate the LCOE of large scale PV power plants at 8 PV plants ranging from 1 to 46 MWp and many similar studies can be found in the literature.

In this section, two objective functions are considered to evaluate the PV power plant performance and to solve its complex design problem. The design variables and constraints of the proposed methodology are also explained.

3.1.1. Objective Function

In this work, the LCOE and maximum annual energy were set as objective functions to determine the optimal solution of the PV plant design. These two objective functions can be combined to form a single optimisation function.

The first part presents the LCOE which is calculated on the basis of the sum of maintenance, operation and installation costs of the plant divided by the total energy generation of the plant during its lifetime. The LCOE method is generally applied to compare power plants with different energy generation sources, by considering the appropriate cost structures. However, the best LCOE for power plants presents the lowest possible investment with high annual energy production. The second part presents the maximum amount of annual energy that can be captured by the PV modules during the PV plant in its lifetime, which is 25 years. The single optimisation function is expressed by the following equation:

$$\min_X \left[\left(\frac{C_c(X) + C_M(X)}{E_{tot}(X)} \right) \cdot a - ((1 - a) \cdot (P_{plant}(X) \cdot n_s \cdot EAF)) \right] \quad (1)$$

where n_s is equal to 1 year.

The optimum values are calculated by using each objective function individually. In other words, in the objective function, a is a binary number; if a is equal to 0, the target of the objective function is maximum energy and, if a is equal to 1, the objective function target is minimum LCOE.

3.1.2. Design Variables

The proposed optimisation algorithm was used for the calculation of all the decision variables, to determine the optimum design of the PV power plant. The chosen optimisation algorithm should have high performance in determining the best design variables and solving the design problem. In this methodology, the proposed decision variables, including the number of PV modules connected

in series (N_s) and parallel (N_p), number of PV module lines per row (N_r), the distance between two adjacent rows (F_y), the tilt angle of the PV module (β), the orientation of PV modules (PV_{orien}), that can be installed vertically or horizontally, optimum PV module (PV_i), and inverter (IN_i), can be selected on the basis of several alternatives from a list of possible candidates.

The vector of the decision variables are summarized as given by the following expression:

$$X = [N_s \ N_p \ N_r \ \beta \ F_y \ PV_{orien} \ PV_i \ IN_i] \quad (2)$$

3.1.3. Constraints

During the design of the PV power plant, many constraints are considered to account for the limits of the different parameters of the whole system. The following expression shows the limitation of some variables:

$$N_{s,min} \leq N_s \leq N_{s,max} \quad (3)$$

$$1 \leq N_p \leq N_{p,max} \quad (4)$$

$$1 \leq N_r \leq N_{r,max} \quad (5)$$

$$0 \leq \beta \leq 90 \quad (6)$$

$$S_{occupied} \leq A_{available} \quad (7)$$

The following equality constraint expressions were used to select the PV module and inverter from the list of candidates:

$$PV_1 + PV_2 + \dots = 1 \quad (8)$$

$$INV_1 + INV_2 + \dots = 1 \quad (9)$$

3.2. System Description and Meteorological Data

This paper focuses on the optimal design of large-scale PV power plants connected to the electric grid. The optimisation process was carried out using HGWOSCA and SCA techniques. The proposed methodology supports PV plant configurations for both central and string topologies and the arrangement of the components within the installation area. Moreover, it considers a list with different types of PV modules and inverters and their specifications as candidates to design the PV power plant, as illustrated in Tables 5 and 6. The actual meteorological data, such as solar irradiance, wind speed, and ambient temperature, are also considered. The optimisation process in this methodology aims to determine the number of PV modules connected in series and parallel, the number of PV module lines per row, the distance between two adjacent rows, the tilt angle of the PV module, the orientation of PV modules that can be installed vertically or horizontally, the optimum PV module and inverter, from a list of possible candidates. Two objective functions, namely the minimum LCOE and maximum annual energy, were considered. Furthermore, the effect of the annual PV module reduction coefficient on PV plant performance was determined.

Table 5. Photovoltaic (PV) modules specifications at standard test condition.

Specification at STC	Unit	PV1	PV2	PV3
Nominal maximum power ($P_{mpp,STC}$)	W	280	285	295
Optimum operating current ($I_{mpp,STC}$)	A	8.84	9.02	9.08
Optimum operating voltage ($V_{mpp,STC}$)	V	31.7	31.6	32.5
Current temperature coefficient (K_i)	(%/C)	0.05	0.05	0.05
Voltage temperature coefficient (K_v)	(%/C)	-0.29	-0.32	-0.29
Open circuit voltage ($V_{oc,STC}$)	V	38.4	38.3	39.6
Wind speed temperature coefficient (K_r)	-	1.509	1.4684	1.509
Length ($L_{pv,1}$)	m	1.65	1.65	1.65
Width ($L_{pv,2}$)	m	0.992	0.992	0.992
Efficiency	%	17.1	17.4	18
Type	-	Mono	Poly	Mono

Table 6. Inverters specifications at standard test condition.

Specification	Unit	INV1	INV2	INV3
Nominal power (P_i)	kW	50	7	500
Minimum input voltage ($V_{i,min}$)	V	250	335	450
Maximum input voltage ($V_{i,max}$)	V	950	560	880
Maximum power point tracking voltage ($V_{i,mppt,max}$)	V	850	540	820
Power loss ($P_{i,sc}$)	W	1.5	1	200
Efficiency (η_{inv})	%	97.5	95.3	98.7

3.2.1. System Description

The architecture of PV plants is composed of several hundreds of PV modules that produce DC power depending on the meteorological parameters (solar radiation and temperature) [64] and inverters that permit the conversion from DC to AC power and ensure the maximum power extraction from the PV modules [65]. The generated power is injected directly into the electric network at the point of common coupling by using step-up transformers [66].

In PV plants, PV modules are connected in series (N_s) to form a string. These strings are rationalised and connected in parallel ($N_p \geq 1$) to form a PV array. In the case of central inverters topology, several hundreds of PV modules are connected to one inverter, and junction boxes need to be used through the DC main cable before leaving for the inverter. In string inverter topology, one string is connected directly to one inverter, and junction boxes need not be placed in the installation field.

The PV arrays within the available area are arranged in multiple rows. Each row consists of multiple lines of PV modules. The number of lines per row is equal to N_r . Considering the shading effect, the inclined adjacent rows are installed with space in between. The tilt angle (β) of PV modules is constant during the PV plant lifetime.

The universal transverse Mercator coordinate (UTM, X: east, Y: north) system was used to model the PV power plant area. Several PV modules vary from one row to another, as the row length varies on the basis of the installation area shape.

3.2.2. Selected Site

The Djanet village is located in the South East of Algerian Sahara in the province of Illizi, and it is characterised by a hot desert climate according to longitude 9.28° E, latitude 24.15° N and an altitude of 1030 m. Djanet village electrification is still dominated by diesel generation (DG). The delivery of fuel leads to an increase in the cost and the maintenance of the units. However, a PV plant grid connected with a capacity of 3 MW was installed in 2015, and its extension is expected to reach 7 MW to supply the village and decrease the units of DG.

3.2.3. Meteorological Data

The performances of PV modules depend on solar irradiation, ambient temperature, and wind speed. These data have been recorded to step times of semi-hourly and hourly. Solar irradiation is expressed in Watts per square meter (W/m^2). Ambient temperature is in degrees Celsius ($^\circ C$). Wind speed is in m/s. Figures 2 and 3 show the daily assessment of the meteorological characteristics. The semi-hourly data of solar irradiance and ambient temperature are observed as more accurate than the hourly data. That is because the peak values of the solar irradiance and ambient temperature may not be recorded in the hourly data. This happens because the data only records point values for every hour, while within a period of time the meteorological data may have significant fluctuation. Thus, semi-hourly data is more precise and accurate compared to hourly data measurements.

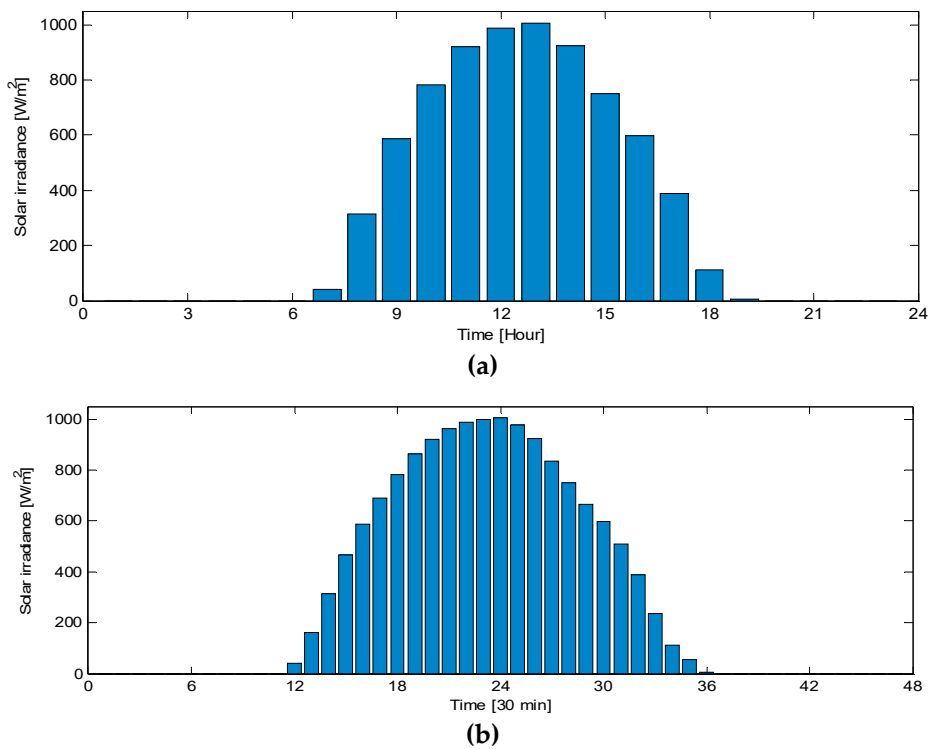


Figure 2. Irradiance data. (a) Hourly average time. (b) 30 min average time.

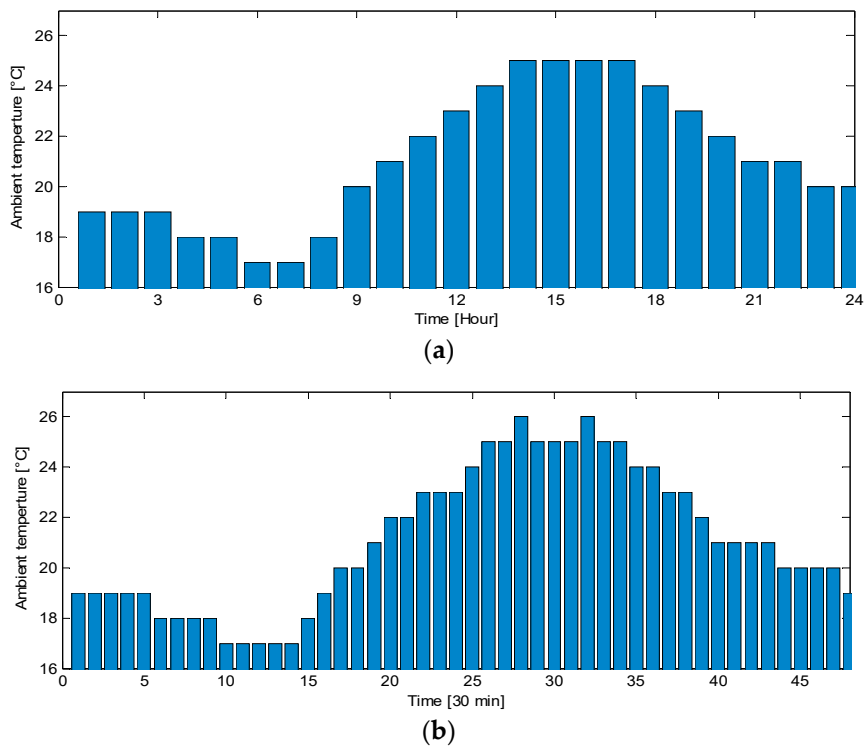


Figure 3. Temperature data. (a) Hourly average time. (b) 30 min average time.

To determine the energy generated by the PV power plant, knowledge of the solar irradiance profile during the year is required. The solar irradiation for hourly and semi-hourly (i.e., 30 min-average) data of the selected location are plotted in Figures 4 and 5. As we can see, the radiation intensity remained high over the year. It is observed that the maximum value of solar irradiance is reached in

March. As for the minimum value of irradiance, this is recorded in June. Each vector represents the same size for 1 year, where the one for semi-hourly step is equal to 17,520 data and the one for hourly step is equal to 8760 data. The climatic conditions of the location are as follows: high solar irradiance potential; ambient temperature with a maximum average of (29.7 °C) in summer; and the sky is mostly clear during the whole year.

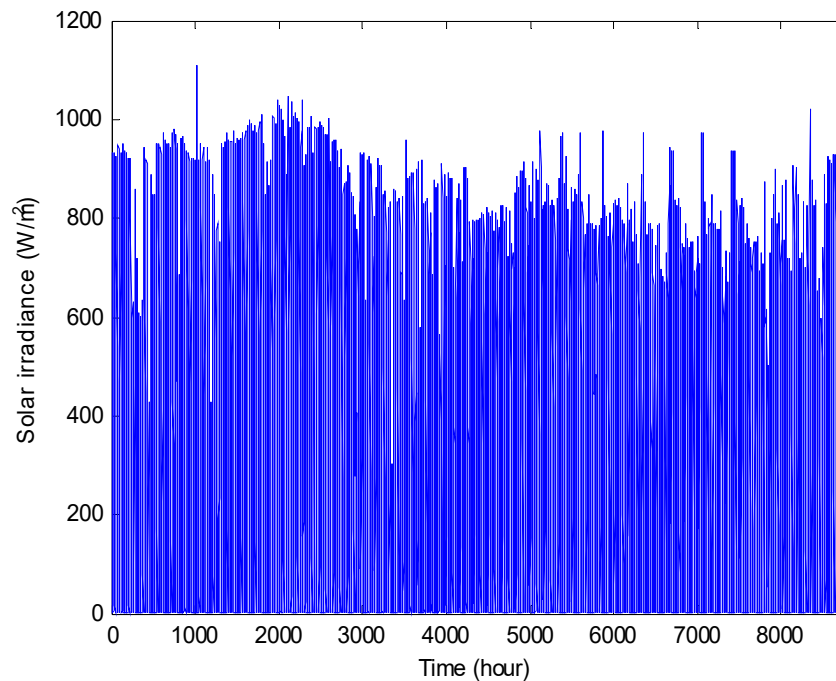


Figure 4. Hourly solar irradiance over the year (W/m^2).

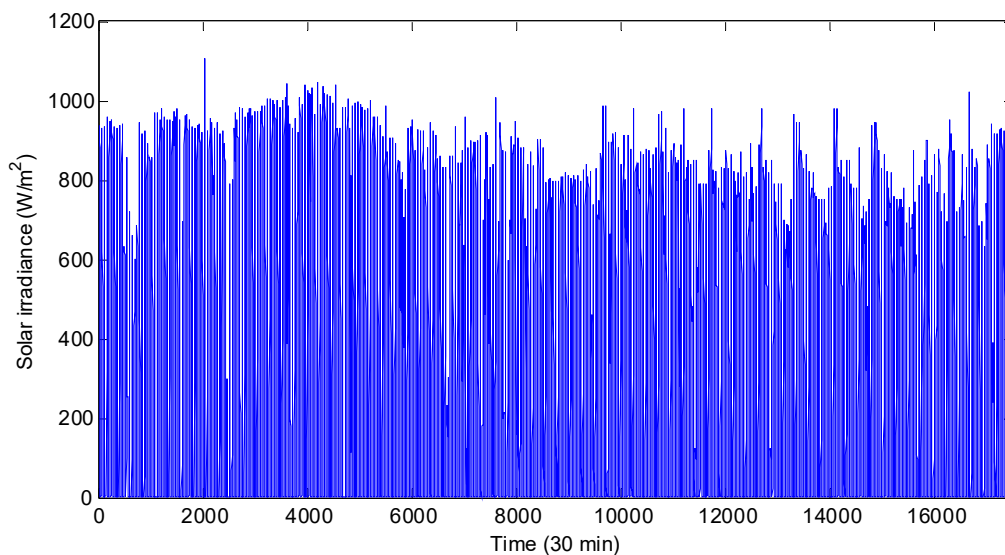


Figure 5. Solar irradiance over the year (W/m^2).

3.3. Proposed Design Methodology

The proposed methodology was applied to solve the PV power plant design and aimed to determine the optimal sizing and configuration of the PV plant, as shown in Figure 6. In the following section, the PV plant design parameters were calculated step by step by considering the measured meteorological data of the location, PV modules, inverter specifications, area coordinates, and cost units.

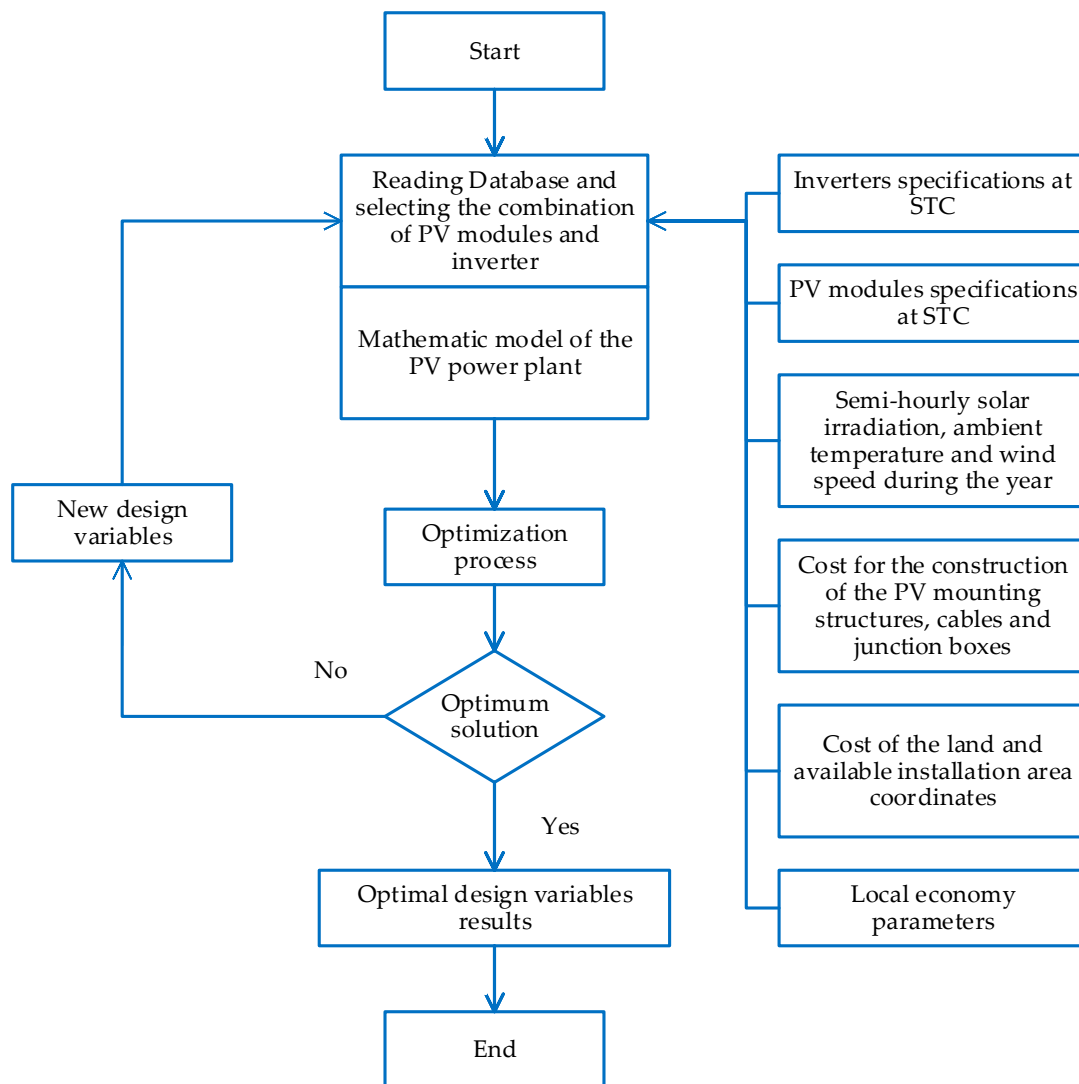


Figure 6. Flowchart of the proposed design methodology.

3.3.1. Irradiance Model

Solar irradiance on tilted PV modules surface is a very important factor in the optimal design of PV power plants. Installation areas with PV modules facing south are suitable for PV power plants [35]. Additionally, a good agreement was shown by PV plants oriented towards the south by using the isotropic model [67].

Several models, which are classified as isotropic and anisotropic, can be used to estimate the solar irradiance on a tilted plane [67,68]. The treatment of diffuse radiation was the only difference between these two models, while the rest is treated the same. However, the isotropic model developed by Liu and Jordan [69] was applied to this methodology to estimate the solar irradiance on the tilted PV module surface [67].

The total radiation received on a horizontal surface (global radiation: I) can be divided into two components: beam and diffused radiation. The estimation of solar radiation on the tilted surface is calculated on the basis of these two components. The total radiation received on the horizontal surface is given by the following equation:

$$I(t) = I_b(t) + I_d(t) \quad (10)$$

The index of transparency of the atmosphere or the clearness index k_T of the sky is an essential factor. The clearness index is the function of the ratio between the extraterrestrial and horizontal radiation, as expressed by the following equation:

$$k_T(t) = \frac{I(t)}{I_0(t)} \quad (11)$$

The diffuse fraction of total horizontal radiation depends on the clearness index of the sky [67] and is expressed by the following equation:

$$\frac{I_d(t)}{I(t)} = \begin{cases} 1.0 - 0.09k_T(t), & k_T(t) \leq 0.22 \\ 0.9511 - 0.1604k_T(t) + 4.388(t)k_T^2 - 16.638k_T^3(t) + 12.336k_T^4(t), & 0.22 < k_T(t) \leq 0.8 \\ 0.165, & k_T(t) \leq 0.80 \end{cases} \quad (12)$$

manipulating Equation (10), the beam radiation is given by the following expression:

$$I_b(t) = I(t) - I_d(t) \quad (13)$$

The total incident solar radiation on tilted surface is the sum of three components, namely, beam radiation from direct radiation of the inclined surface, diffuse radiation and reflected radiation.

$$I_T(t, \beta) = I_B(t) + I_D(t) + I_R(t) \quad (14)$$

The beam irradiance on an inclined surface can be calculated on the basis of multiplication between beam horizontal irradiance and beam ratio factor R_b , as shown in the following expression:

$$I_B(t) = I_b(t)R_b(t, \beta) \quad (15)$$

where the beam ratio factor R_b is a function of the ratio between beam irradiance on the inclined surface and horizontal irradiance, as expressed in the Equation (18).

The first component is the incidence angle $\cos(t, \beta)$, which can be derived as follows:

$$\begin{aligned} \cos(t, \beta) &= \sin \delta(t) \sin \varphi \cos \beta - \sin \delta(t) \cos \varphi \sin \beta \cos \gamma \\ &\quad + \cos \delta(t) \cos \varphi \cos \beta \cos \omega(t) \\ &\quad + \cos \delta(t) \sin \varphi \sin \beta \cos \gamma \cos \omega(t) \\ &\quad + \cos \delta(t) \sin \beta \sin \gamma \sin \omega(t) \end{aligned} \quad (16)$$

where δ is the solar declination angle, φ is the location latitude, γ is the surface azimuth angle, and ω is the hour angle. The global radiation on the inclined surface calculation model's error was lower than 3% [70].

The second component deals with solar zenith angle $\cos \theta_z$ and can be calculated using the following equation:

$$\cos \theta_z(t, \beta) = \cos \gamma \cos \delta(t) \cos \omega(t) + \sin \varphi \sin \delta(t) \quad (17)$$

$$R_b(t, \beta) = \frac{\cos(t, \beta)}{\cos \theta_z(t, \beta)} \quad (18)$$

Diffuse irradiance on an inclined surface is computed on the basis of the isotropic sky model. A well-known isotropic model was introduced by Liu and Jordan (1963). This model is simple, and the diffuse radiation has a uniform distribution over the skydome. The diffuse radiation on the inclined surface increases with an increasing amount of seen by the inclined surface, as expressed in Equation (19).

$$I_D(t) = I_d(t) \left(\frac{1 + \cos \beta}{2} \right) \quad (19)$$

where β is the surface tilt angle and considered as a design variable. Its optimal values are computed by the optimisation algorithm.

The reflected irradiance on an inclined surface is expressed by Equation (20) and depends on the transposition factor for ground reflection R_r given by Equation (21) and the reflectivity of the ground ρ that is equal to 0.2 [68].

$$I_R(t) = I(t)\rho R_r \quad (20)$$

$$R_r(t) = \frac{1 - \cos\beta}{2} \quad (21)$$

3.3.2. Area Calculation Model

In actual cases, the PV power plant installation area is limited in surface and does not have a uniform shape. However, this proposed methodology can be applied to all actual area shapes to determine the optimal size and configuration of large-scale PV power plants. This methodology supports actual area shapes by using the coordinates of the location under study. Additionally, the universal transverse Mercator coordinate (UTM, X: east, Y: north) system is used to model the PV power plant area. Furthermore, the PV plant occupying the surface, length, and width of each row, junction boxes, and cable length are computed on the basis of the coordinates. As mentioned in the previous section, PV nodules are oriented towards the south in the installation field, as illustrated in Figure 7.



Figure 7. Arrangement of PV modules according to PV plant shape.

The Y-axis was used to calculate the total number of rows supported by the PV plant area and the width (W_T) of each row. The space between two adjacent rows (F_y), which is a design variable, and its optimum value were calculated by the algorithm process. The following equation expresses the total number of rows:

$$N_{row} = \text{floor}\left(\frac{\max(Y) - \min(Y)}{W_T + F_y}\right) \quad (22)$$

After calculating the total number of rows (N_{row}), it can be used to calculate the north coordinates of each row (Y_{Ni}) in the PV plant, as expressed in the following equation:

$$Y_{Ni} = \min(Y) + (W_T + F_y)N_i \quad (23)$$

The parameters (N_i) and (Y_{Ni}) are subject to a constraint in this methodology, as provided in Equations (24) and (25):

$$1 \leq N_i \leq N_{row} \quad (24)$$

$$\min(Y) < Y_{Ni} < \max(Y) \quad (25)$$

The X-axis presents the east coordinates and is used for calculating the length of each row in the PV plant X_{Ni} , as expressed in the following straight-line equation:

$$X_{Ni} = \frac{(X_2 - X_1)(Y_{Ni} - Y_1)}{Y_2 - Y_1} + X_1 \quad (26)$$

where (X_1, Y_1) and (X_2, Y_2) correspond to the coordinates of two consecutive points. The parameter X_{Ni} is a constraint in this methodology, as provided in the following expression:

$$\min(X) \leq X_{Ni} \leq \max(X) \quad (27)$$

The row length (M_{row_i}) is obtained after the calculation of the east coordinates (X_{Ni}) of each row, considering the difference between these coordinates, and is expressed by using Equation (28):

$$M_{row_i} = X_{Ni1} - X_{Ni2} \quad (28)$$

The PV power plant area calculation process considers other important parameters, such as row height (H_T), row width (W_T) and the space between two adjacent rows (F_y). These parameters can be calculated on the basis of the following equations:

$$W_T = N_r L_{pv,2} \cos \beta \quad (29)$$

$$H_T = N_r L_{pv,2} \sin \beta \quad (30)$$

$$F_y = dH_T \quad (31)$$

where (N_r) and (F_y) are considered as design variables, and their optimal values are calculated via optimisation. Notably, (N_r) is the number of PV module lines in each row, and (F_y) is the distance between two adjacent rows. In this methodology, all rows in the installation area have the same lines of PV modules. The arrangement of rows and PV modules in a row within the installation area is shown in Figure 7.

3.3.3. Components Arrangement

The arrangement of the components within the installation area is an essential part of the PV plant design process in the presence of several parameters, such as the location characteristics and the device's specifications. In addition, component arrangement depends on the optimal topology selected by the optimisation algorithm. Furthermore, the distribution of a large amount of the components among the PV power plant is computed in terms of several constraints.

However, PV modules and inverters are the two main devices considered in the PV power plant arrangements. Additionally, in case of the optimisation algorithm select central topology, the junction box arrangement is considered, and its distribution among the PV modules and the inverters is calculated on the basis of its rating power.

Finally, the PV power plant device arrangement is influenced by the amount of solar irradiance, ambient temperature, wind speed, and the geographic location. These parameters affect the tilt angle of PV modules and increase or decrease the PV module energy output, leading to the installation of varying numbers of inverters in the PV plant. Moreover, in this methodology, the aforementioned parameters are considered to control the total cost.

Dependent on PV inverter size, the number of series PV modules in each string (N_s) and parallel PV modules (N_p) should be computed by the algorithm to meet a specific voltage and current requirement of inverters. On the one hand, to avoid the inverter damage that can be caused by overvoltage in case of low temperature in some locations, in every string, the number of PV modules connected in series

has to be optimally computed. On the other hand, the number of parallel-connected PV modules (N_p) multiplied by its current is equal to the input current of the inverter. To avoid the inverter damage created by the overcurrent locations with high solar irradiance, a limited number of PV modules connected in parallel (N_p) should be addressed.

The first part handles PV modules distribution among the inverters and their arrangement within the PV plant area. The number of series (N_s) and parallel (N_p) PV modules are computed in accordance with the optimum selected inverter by the optimisation process. In this proposed methodology, the number of PV modules connected in series (N_s) and parallel (N_p) were considered as the design variables, and their optimum values were calculated using the optimisation algorithm. The (N_s) design variable involves a number of minimum ($N_{s,min}$) and maximum ($N_{s,max}$) PV modules, and these limitations can be calculated on the basis of the inverter input voltage range in [11,22], as expressed in the following equations:

$$N_{s,min} = \frac{V_{i,min}}{V_{mpp,min}} \quad (32)$$

$$N_{s,min} = \frac{V_{i,max}}{V_{oc,max}} \quad (33)$$

$$N_{sm,2} = \frac{V_{i,mpp,max}}{V_{mpp,max}} \quad (34)$$

$$N_{s,max} = \begin{cases} N_{sm,1}, N_{sm,1} \leq N_{sm,2} \\ N_{sm,2}, N_{sm,2} < N_{sm,1} \end{cases} \quad (35)$$

The maximum number of PV modules connected in parallel (N_p) was calculated according to the selected inverter by using the nominal power (P_i), and the PV module maximum output power ($P_{mpp,max}$) was selected with respect to the optimum number of PV modules connected in series (N_s) [22], as provided in the following expression:

$$N_{p,max} = \frac{P_i}{N_s P_{mpp,max}} \quad (36)$$

As mentioned in the previous section, the arrangement of PV modules in the PV plant area requires the use of the length of each row in the PV plant to determine the optimum number of PV modules installed in each line (N_{c_i}) and the total number in each row ($N_{row_i,pv}$). The total number of PV modules installed in each line (N_{c_i}) of rows, which are described as the function ratio between the length of each row (M_{row_i}) and the length of the optimum PV modules ($L_{pv,1}$), is given in the following equation:

$$N_{c_i} = \frac{M_{row_i}}{L_{pv,1}} \quad (37)$$

The total number of PV modules installed in each row ($N_{row_i,pv}$) depends on the number of PV module lines (N_r), which is a design variable in this methodology, and its optimum value is computed by the optimisation algorithm.

$$N_{row_i,pv} = N_r N_{c_i} \quad (38)$$

The sum of PV modules in each row of the PV plant results in their total number in the installation area as expressed in the following equation:

$$N_I = \sum_1^i N_{row_i,pv} \quad (39)$$

The number of series (N_p) and parallel (N_p) PV modules are the main parameters in the inverter calculation process. These design variables determine the number of blocks, and x_{inv} represents the pieces of inverters in blocks, and each piece is composed of N_{block} [22], as given in the following equations:

$$N_{block} = N_s N_p \quad (40)$$

$$y = (N_i, N_{block}) \quad (41)$$

$$x_{inv} = \frac{N_i - y}{N_{block}} \quad (42)$$

Finally, the total number of inverters is calculated on the basis of the following expression:

$$N_i = \begin{cases} x_{inv} \left(\frac{y}{x_{inv}} \right) P_{pv, stc} \leq 0.1 P_i \\ x_{inv} + 1, \left(\frac{y}{x_{inv}} \right) P_{pv, stc} > 0.1 P_i \end{cases} \quad (43)$$

3.3.4. PV Plant Total Energy

The proposed methodology offers many alternatives for PV modules with different specifications. Additionally, the optimisation algorithm was applied to determine the best candidate for the design of the PV plant and the optimum configuration of the PV plant as a global solution. However, the PV module output power depends on the amount of solar radiation, ambient temperature, wind speed, and electrical characteristics. Moreover, a recent review [71] has covered approximately 70 important papers on PV cell modelling, and the equations used in this proposed methodology have been applied in several papers, as shown in this review. The equations have been used in a recent paper [72], and the obtained results by the proposed procedure are more accurate than the [73] model, which involves the use of the same equations. Accordingly, these equations are suitable for calculating the performance of PV modules in our proposed design procedure.

The PV power plant consists of a large number of PV modules. Additionally, the output power is assumed to be the same for all PV modules in the PV plant, except for the southernmost row, which is considered never shaded. More importantly, the degradation of PV modules is inevitable regardless of the size of a PV power plant [74,75]. However, this research considered the PV module output power derating factor (d_f) due to soiling effect on the PV module surface, which is equal to $d_f = 0.069$, and the annual reduction coefficient r of PV module [34], which is equal to 0.5%. Finally, PV modules output power can be calculated using the following expression:

$$P_{pv}(t, \beta) = (1 - r)(1 - d_f) P_{mpp}(t, \beta) \quad (44)$$

where P_{mpp} presents the produced power by each PV module in the PV plant.

The produced energy can be affected by the shadow area on PV modules and is related to the shade impact factor (SIF) [76], and its value is equal to 2 [35]. This parameter can be obtained using the following equation:

$$A_{S_i}(t) = \xi_i(t) SIF \quad (45)$$

where ($\xi_i(t)$) presents the ratio of the shadow area.

The total energy of the PV power plant can be calculated according to the optimum inverter topology selected by the optimisation algorithm. Furthermore, the PV power plant produced energy and the total cost can be influenced by the selected inverter topology. For string inverter topology, the following equation is applied to calculate the PV plant output power:

$$P_{plant}(t, \beta) = n_{tr}(1 - \eta_{cac})(1 - \eta_{cic}) P_{o_i}(t, \beta) N_i \quad (46)$$

where (P_{o_i}) is the inverter output power, (N_i) represents the total number of inverters, (n_{tr}) is the transformer efficiency, (η_{cac}) presents the AC cable losses and (η_{cic}) is the interconnection cable losses.

In the case of central inverter topology, PV plant output power can be obtained using the following equation:

$$P_{\text{plant}}(t, \beta) = (1 - \eta_{cdc})n_{m\text{ppt}}n_{inv}n_{tr}(1 - \eta_{cac})(1 - \eta_{cic}) \sum_1^{\text{row}_i} P_{\text{row}_i}(t, \beta) \quad (47)$$

where $P_{\text{row}_i}(t, \beta)$ presents the PV row output power, $n_{m\text{ppt}}$, n_{inv} and n_{tr} are the efficiencies of the PV module, inverter and transformer, respectively, and η_{cdc} and η_{cac} , are the DC and AC cable losses, respectively.

However, in this methodology, the PV plant energy generation was directly injected to the electric network over its operational lifetime, and it was calculated using Equation (48):

$$E_{\text{tot}} = P_{\text{plant}}(t, \beta)n_s\text{EAF} \quad (48)$$

where EAF is the energy availability factor, and (n_s) is the PV plant operational lifetime.

3.3.5. PV Plant Total Cost

The PV power plant consists of two types of costs, as expressed by Equation (49):

$$C_{\text{tot}} = C_c + C_M \quad (49)$$

The installation cost (C_c) deals with the cost of the device, such as C_{pv} , C_{inv} which represents the unit cost of the PV modules and inverters, respectively. In addition, C_B is the PV module mounting structure cost. Moreover, C_{cb} , C_{tr} , C_{pd} , and C_{cm} represent the costs of the cable, transformer, protection devices and monitoring system, respectively. Finally, C_L represents the cost of the plant area. The installation cost is expressed in Equation (50):

$$C_c = N_I C_{pv} + N_i C_{inv} + C_L + C_B + C_{cb} + C_{tr} + C_{pd} + C_{cm} \quad (50)$$

The operation and maintenance costs of the PV plant during its lifetime depend on the annual inflation rate (g), the nominal annual interest rate (i_r). and the operation and maintenance costs per watt (M_{op}), as given in the following expression:

$$C_M = N_I P_{pv, \text{stc}} M_{op} (1 + g) \left[\frac{1 - \left(\frac{1+g}{1+i_r}\right)^{n_s}}{i_r + g} \right] \quad (51)$$

4. Hybrid Grey Wolf Optimizer-Sine Cosine Algorithm (HGWOSCA)

SCA and grey wolf optimiser (GWO) are meta-heuristic optimisation algorithms recently developed by Mirjalili et al. [44,77]. Both SCA and GWO approaches show high performance compared with other well-known meta-heuristic algorithms [44,77]. The hybrid GWO-SCA technique was introduced by N. Singh et al. [43] for combining the advantages of both approaches. In the GWO-SCA hybrid approach, GWO presents the main part, whereas the implementation of SCA assists in the optimisation of GWO. An improvement in the position, speed, and convergence of the best grey wolf individual alpha (α) by using the original equation expressed in [77], is achieved by applying the position updating equations of the SCA approach, as illustrated in [44].

The position of the current space agent is updated on the basis of the following equation:

$$\vec{x}_2 = \vec{x}_\beta - \vec{a}_2 \cdot (\vec{d}_\beta), \vec{x}_3 = \vec{x}_\delta - \vec{a}_3 \cdot (\vec{d}_\delta) \quad (52)$$

where \vec{a} is random value in the gap $[-2a, 2a]$.

The position of \vec{X}_β , \vec{X}_δ , and \vec{X}_α is updated using the following equation:

$$\frac{\vec{x}_1 + \vec{x}_2 + \vec{x}_3}{3} \quad (53)$$

Details and description of the HGWOSCA approach can be found in reference [43]. Furthermore, the computational procedure of the HGWOSCA approach is illustrated in Figure 8.

1.	Begin of Algorithm
2.	Initialize the grey wolf population $x_i = 1, 2, \dots, n$
3.	Initialize the parameters A , a and C
4.	Calculate the fitness of each search agent
5.	\vec{X}_α = the best search agent
6.	= the second best search agent
7.	\vec{X}_δ = the third best search agent
8.	While $t < \text{Max_generation}$
9.	For search space
10.	Update the position of the current space agent in the basis of equation (53)
11.	End
12.	Update the parameters a , A and C
13.	Calculate the fitness of search agent
14.	Update the \vec{X}_β , \vec{X}_δ by equation (52) and \vec{X}_α as below
15.	if $\text{rand}() < 5$
16.	then
17.	$\vec{D}_\alpha = \text{rand}() \times \sin(\text{rand}()) \times + \vec{C}_1 \cdot \vec{X}_\alpha - \vec{X} $
18.	else
19.	$\vec{D}_\alpha = \text{rand}() \times \cos(\text{rand}()) \times + \vec{C}_1 \cdot \vec{X}_\alpha - \vec{X} $
20.	$\vec{X}_1 = \vec{X}_\alpha - \vec{A}_1 \cdot \vec{D}_\alpha$
21.	end if
22.	end else
23.	end while
24.	Return \vec{X}_α

Figure 8. Pseudo-code of the hybrid grey wolf optimiser-sine cosine algorithm (HGWOSCA).

Although the GWO and SCA are able to expose an efficient accuracy in comparison with other well-known swarm intelligence optimisation techniques, it is not fitting for highly complex functions and may still face the difficulty of getting trapped in local optima [43]. Thus, a new hybrid variant based on GWO and SCA is used to solve recent real-life problems.

5. Results and Discussion

The proposed methodology has been implemented in MATLAB software and applied to the development of the optimal design of a PV plant connected to the electric grid. Solar irradiance, ambient temperature, and wind speed data for 1 year from the installation field are required. The effect of minimum LCOE and maximum annual energy objective functions on the PV plant design was determined. The HGWOSCA optimisation technique and a single SCA algorithm were applied with 400 search agents and 30 iterations to solve the design problem.

According to the results presented in Table 7, the PV plant optimal design variables depend on the selected objective function. The minimum LCOE and maximum annual energy result in two completely different optimal PV plant structures. PV power plant results are presented in

Table 8. The optimisation process applying HGWOSCA outperforms the single SCA for minimum and maximum objective functions.

Table 7. Optimal design variables using semi-hourly measurement data.

Design Variables	Minimum Levelised Cost of Energy (LCOE)		Maximum Energy	
	Sine Cosine Algorithm (SCA)	HGWOSCA	SCA	HGWOSCA
N_s	20	18	21	16
N_p	70	74	49	62
N_r	5	4	1	1
β	15	15	15	15
F_y	1.925	1.542	0.640	0.643
PV_i	PV1	PV3	PV3	PV3
INV_i	INV3	INV3	INV3	INV3
PV_{orien}	1	1	2	2

Table 8. Results of optimal design algorithms using semi-hourly measurement data.

PV Plant Parameters	Minimum LCOE		Maximum Energy	
	SCA	HGWOSCA	SCA	HGWOSCA
LCOE (\$/MWh)	29.1829	28.6283	32.0983	32.1174
Yearly total energy (MWh)	731.4199	776.4012	785.8698	786.5035
Total energy (GWh)	18.2855	19.410	19.6467	19.6626
Total cost (M\$)	0.5336	0.5557	0.6305	0.6315
Installation Cost (M\$)	0.4465	0.4632	0.5368	0.5378
Maintenance cost (M\$)	0.0871	0.0925	0.0936	0.0937
Junction Boxes	6	7	18	18
PV modules (N_I)	1365	1376	1393	1394
Inverters (N_i)	1	1	2	2
Rows	11	14	36	36

For both objectives using HGWOSCA, the optimisation process has selected mono-crystalline PV module type 3 (PV3) from the list of candidates. This module uses 295 W, and inverter type 3 (INV3) was selected from a list of three inverters. This inverter uses 500 kW and presents the central topology of the PV power plant. With the objective of maximum annual energy, the suggested number of PV modules is 1394 and 2 inverter to have 786.5035 (MWh). In this case, the LCOE was 32.1174 (\$/MWh), and the PV plant total cost was the highest at 0.6315 (M\$). With the objective of minimum LCOE, the number of PV modules is 1376 and only 1 inverter is required to have 28.6283 (\$/MWh) of LCOE. In this case, the annual energy generation is equal to 786.5035 (MWh), and the total cost was reduced to 0.5557 (M\$) compared with the first case. The use of LCOE's objective function to optimise the design of PV plants can reduce the financial risks, as proven in this case study. The total cost of using minimum LCOE decreased by 12% with a benefit of 71,800 (\$) in terms of installation cost, maintenance and operation costs. Figure 9 illustrates the maintenance and operational costs and the installation cost throughout the life of the PV plant for minimum LCOE and maximum annual energy generation.

The area occupied by the PV power plant can be calculated based on the summation of the occupied area by all PV rows, according to the length of each row and the inter-row area of all adjacent rows. The total available area of the installation field is equal to 3131 m² and the installed PV modules occupied 3094 m² of the installation site, which is nearly the same as the total area of the field. Therefore, the percentage of the occupied area by PV modules in the two cases presents 99% of the available area. The arrangement of PV modules in rows within the installation area is illustrated in Figure 10 using the LCOE objective function. The length of each row changed from one row to another according to the shape of the PV plant. Furthermore, this configuration has been designed in terms of the shape of the installation area, reflecting the actual situation. The difference obtained on the energy production

using LCOE and maximum energy objective functions is due to the configuration and the arrangement of the PV modules within the available installation area. On the one hand, the optimal design of the PV plant under the maximum annual energy resulted in the minimum number of lines N_r installed in each row, which is equal to 1. Additionally, this arrangement allowed the PV modules to capture more reflected radiation from the ground. Furthermore, at $N_r = 1$, a small distance between two adjacent rows in terms of shading effect is required, thereby increasing the total number of rows in the installation area to $D_{row} = 36$ with one PV module line in each row and increasing the reflected radiation on PV modules. Moreover, the total number of PV modules for maximum energy is equal to 1394 and distributed among two central inverters. However, the number of PV modules for LCOE is less, leads to 1379 and arranged among only one inverter. PV modules are installed in multiple lines in case of LCOE objective function. In this configuration, the number of lines N_r for each row is equal to 4 and leads only to 14 rows. Moreover, this configuration decreases the reflected radiation from the ground to be captured by PV modules and cannot be absorbed by the rest of the lines ($N_r > 1$). The PV modules are installed horizontally for minimum LCOE ($PV_{orien} = 1$) and vertically ($PV_{orien} = 2$) for maximum annual energy.

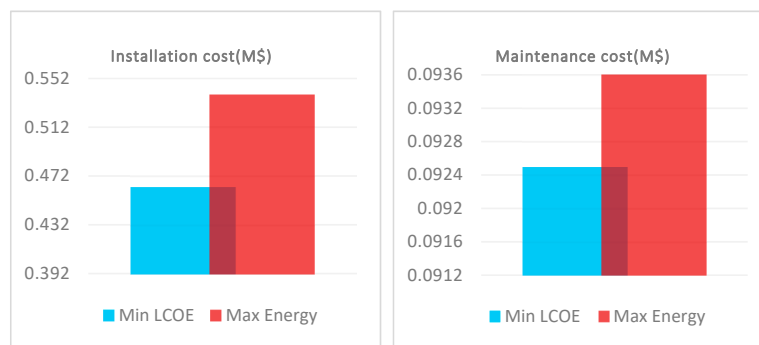


Figure 9. Throughout the life of the PV plant optimised by HGWOSCA.

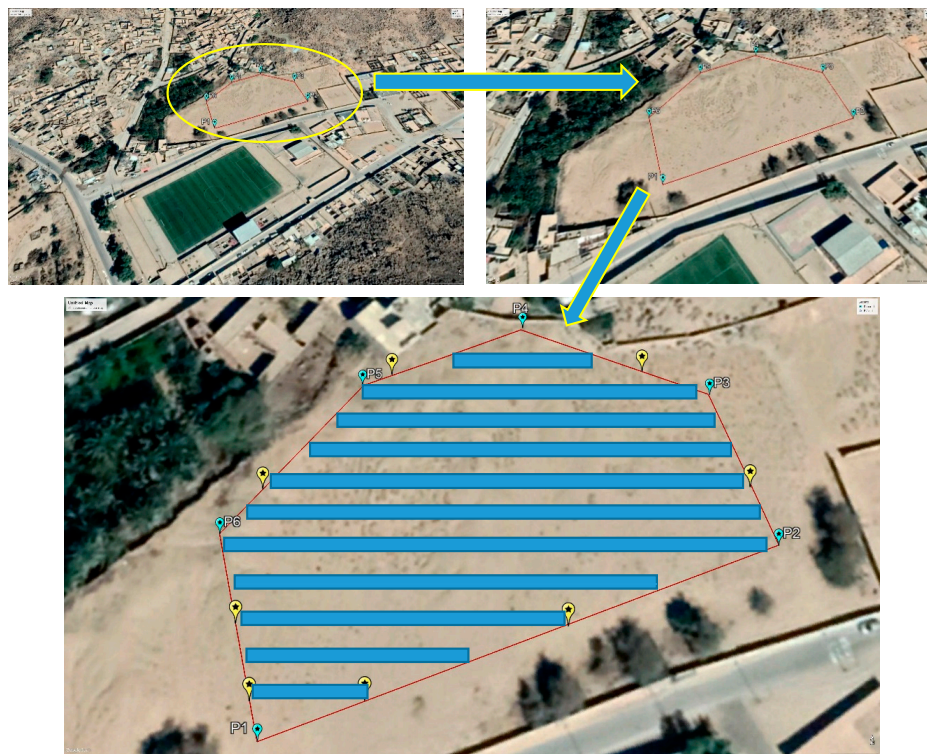


Figure 10. Rows arrangement for minimum LCOE using HGWOSCA.

Figure 11 illustrates the monthly energy generation by the PV power plant for the LCOE objective function. The PV plant energy generation remained high over the year, with an energy average of 65 (MWh) per month. The highest value of the energy generated by the PV power plant is obtained in March, because this condition is due to the high solar irradiance in this period.

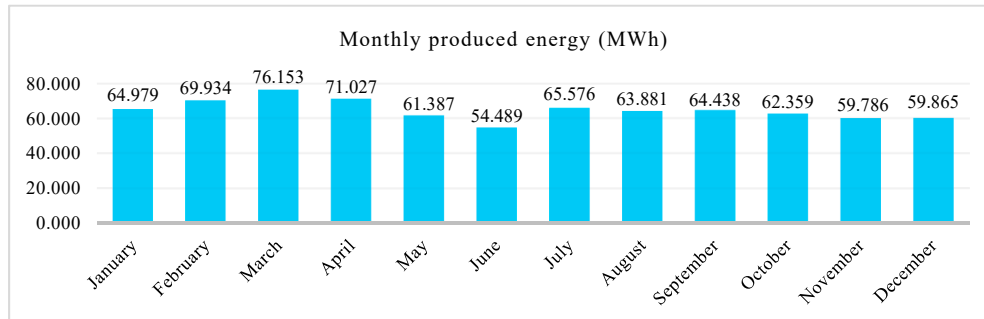


Figure 11. PV plant energy generation (MWh).

For comparison, the semi-hourly average time was compared with the hourly average time meteorological data to examine the step time effect on the PV plant performance. The peaks of the meteorological data can influence the design solution. Therefore, the usage of annual semi-hourly average time rather than monthly, daily and hourly is recommended, as semi-hourly data contain the troughs and peaks of solar irradiation, ambient temperature, and wind speed. According to the results presented in Tables 9 and 10, the step time data can affect the objective functions. The LCOE for semi-hourly average time is 28.6283 (\$/MWh), and that obtained for hourly average time is higher and equal to 28.637 (\$/MWh). The use of semi-hourly average time meteorological data in designing the PV plant can increase the financial benefits.

Table 9. Optimal design variables using hourly measurement data.

Design Variables	Minimum LCOE		Maximum Energy	
	SCA	HGWOSCA	SCA	HGWOSCA
N_s	19	18	22	14
N_p	70	74	42	47
N_r	5	4	1	1
β	15	15	15	15
F_y	1.925	1.540	0.64	0.64
PV_i	PV3	PV3	PV3	PV3
INV_i	INV3	INV3	INV3	INV3
PV_{orien}	1	1	2	2

Table 10. Results of optimal design algorithms using hourly measurement data.

PV Plant Parameters	Minimum LCOE		Maximum Energy	
	SCA	HGWOSCA	SCA	HGWOSCA
LCOE (\$/MWh)	28.6622	28.6370	32.0983	32.1552
Yearly total energy (MWh)	770.0032	776.1651	785.6774	786.2915
Total energy (GWh)	19.2501	19.4041	19.6419	19.6573
Total cost (M\$)	0.5517	0.5557	0.6305	0.6321
Installation Cost (M\$)	0.4600	0.4632	0.5368	0.5384
Maintenance cost (M\$)	0.0917	0.0925	0.0936	0.0937
Junction Boxes	6	7	18	18
PV modules (N_I)	1365	1376	1393	1394
Inverters (N_i)	1	1	2	2
Rows	11	14	36	36

In all resulting cases, the proposed HGWOSCA optimisation approach was applied successfully and showed higher efficiency than that of a single SCA technique, with high performance in determining the optimal solution and solving the PV plant complex design problem. The convergence optimisation of annual energy and LCOE is illustrated in Figures 12 and 13.

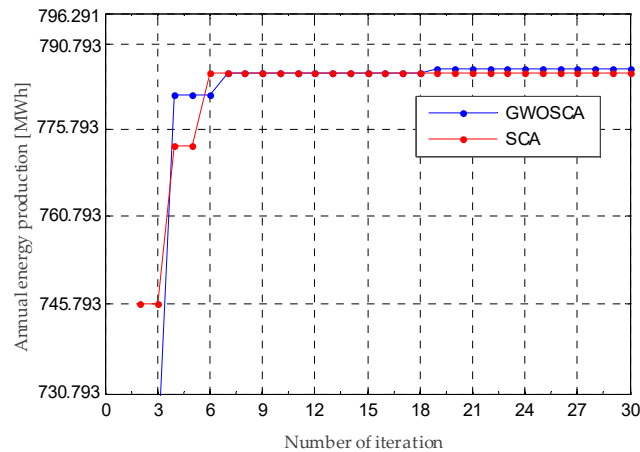


Figure 12. Convergence of the optimisation of annual energy using HGWOSCA algorithm for semi-hourly data.

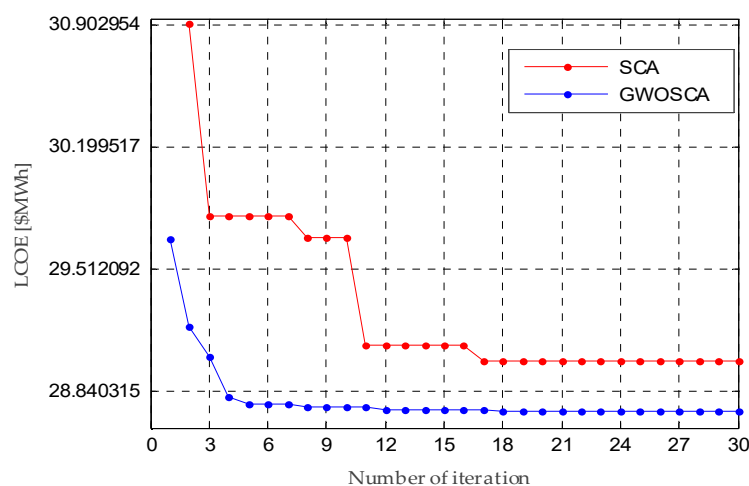


Figure 13. The convergence of the optimisation of LCOE using HGWOSCA algorithm for semi-hourly data.

Effect of PV Module Reduction Coefficient

A sensitivity analysis was applied to evaluate the PV power plant performance. Accordingly, the variations in the PV module annual reduction coefficient were investigated. The optimisation results were obtained for different annual reduction coefficient values, from 0.3% to 0.7% per year. The annual reduction coefficient used in this study was 0.5%, as mentioned in Equation (44).

The optimum results for five different values for the annual reduction coefficient of the PV module are presented in Figures 14 and 15. According to the results, by increasing the PV module reduction coefficient, the PV plant energy production is reduced throughout its lifetime period. The LCOE of the PV plant increases by increasing the PV module reduction coefficient. By contrast, the total cost of the PV power plant is not affected and has the same value for all reduction coefficient values.

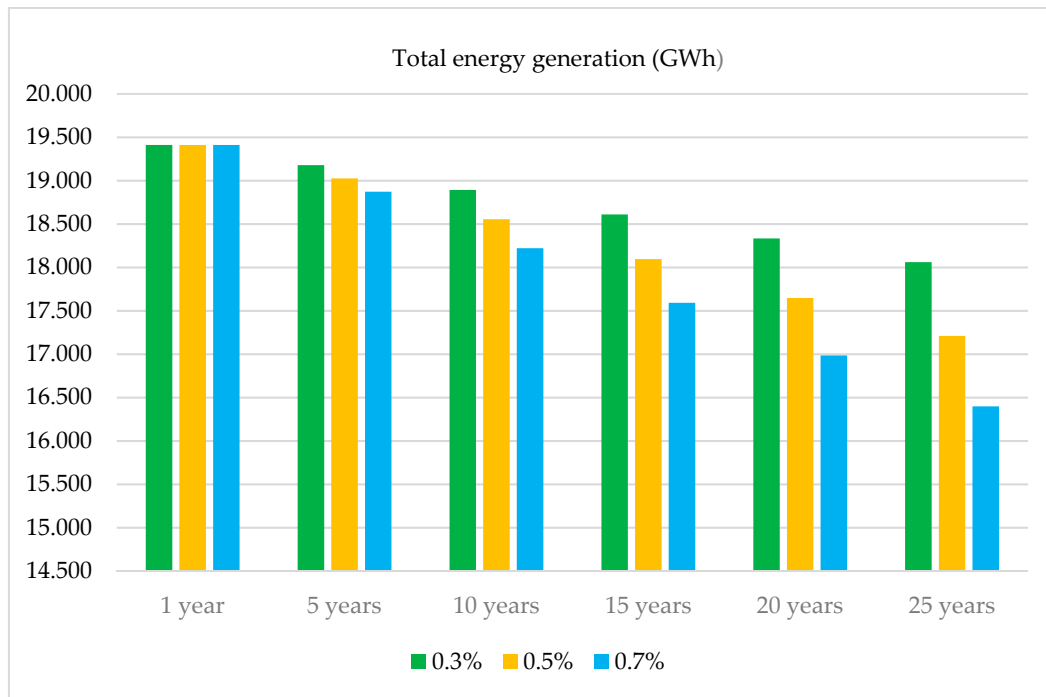


Figure 14. Total energy for reduction coefficient variations.

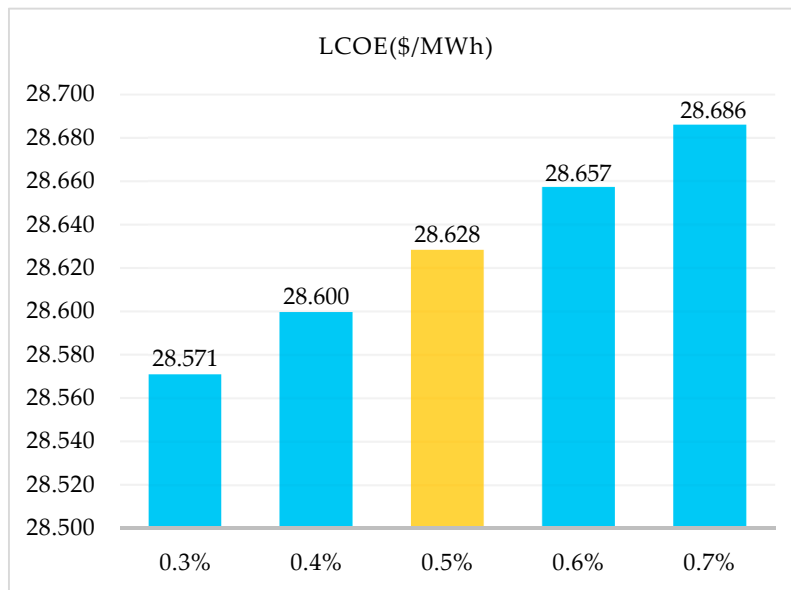


Figure 15. LCOE for reduction coefficient variations.

In economic terms, an improved PV module annual reduction coefficient leads to the recovery of capital investment of the PV plant within a smaller time period, making the PV plant economically profitable. Moreover, the sensitivity of the PV power plant improved by the decrement of the PV module annual reduction coefficient and vice versa.

6. Conclusions

The proposed methodology was executed using semi-hourly time-resolution (i.e., 30 min-average) values of meteorological input data, including solar irradiance, ambient temperature, and wind speed. The procedure considers PV modules and inverter specifications, including a list of different

commercially available PV modules and inverter technologies as candidates. The optimisation process selects only one PV module and inverter from a list of several alternatives, presenting the optimum combination. The proposed PV plant area model considers the shape and size of the installation field to properly arrange all the existing components.

The minimum LCOE and maximum annual energy objective functions were used to design the PV power plant. On the basis of the optimal results, the total cost of using the minimum LCOE objective function decreased by 12% with a benefit of 71,800 (\$), including installation cost and maintenance and operation costs compared with the maximum annual energy. In this methodology, the HGWOSCA optimisation technique and a single SCA algorithm were applied. The optimum design solution shows that the proposed HGWOSCA is more efficient. Additionally, the PV plant optimal design variables depend on the selected objective function. The minimum LCOE and maximum annual energy result in two different optimal PV plant structures. LCOE improved with the use of semi-hourly average time meteorological data for designing the PV plant and can increase the financial benefits. Moreover, the sensitivity analysis shows that the PV power plant can be improved by the decrement of the PV module annual reduction coefficient and makes the PV plant economically more profitable.

Author Contributions: T.E.K.Z. contributed theoretical approaches, simulation, and preparing the article; M.R.A., M.F.N.T., S.M.Z. and A.D. contributed to supervision; M.R.A., A.D. and S.M. contributed to article editing. All authors have read and agreed to the published version of the manuscript.

Funding: This research was funded by the School of Electrical System Engineering Research Fund (SESERF), UniMAP.

Acknowledgments: We gratefully acknowledge the support of the Algerian company of electricity SONELGAZ, for providing the measurement data.

Conflicts of Interest: The authors declare no conflict of interest.

References

1. Mohammadi, K.; Naderi, M.; Saghafifar, M. Economic feasibility of developing grid-connected photovoltaic plants in the southern coast of Iran. *Energy* **2018**, *156*, 17–31. [[CrossRef](#)]
2. Zou, H.; Du, H.; Brown, M.A.; Mao, G. Large-scale PV power generation in China: A grid parity and techno-economic analysis. *Energy* **2017**, *134*, 256–268. [[CrossRef](#)]
3. Feldman, D.; Margolis, R. *Q2/Q3 2018 Solar Industry Update 2018*; Technical Report; National Renewable Energy Lab. (NREL): Golden, CO, USA, 2018.
4. Comello, S.; Reichelstein, S.; Sahoo, A. The road ahead for solar PV power. *Renew. Sustain. Energy Rev.* **2018**, *92*, 744–756. [[CrossRef](#)]
5. Mondol, J.D.; Yohanis, Y.G.; Norton, B. Optimal sizing of array and inverter for grid-connected photovoltaic systems. *Sol. Energy* **2006**, *80*, 1517–1539. [[CrossRef](#)]
6. Kornelakis, A.; Marinakis, Y. Contribution for optimal sizing of grid-connected PV-systems using PSO. *Renew. Energy* **2010**, *35*, 1333–1341. [[CrossRef](#)]
7. Notton, G.; Lazarov, V.; Stoyanov, L. Optimal sizing of a grid-connected PV system for various PV module technologies and inclinations, inverter efficiency characteristics and locations. *Renew. Energy* **2010**, *35*, 541–554. [[CrossRef](#)]
8. Sulaiman, S.I.; Rahman, T.K.A.; Musirin, I.; Shaari, S.; Sopian, K. An intelligent method for sizing optimization in grid-connected photovoltaic system. *Sol. Energy* **2012**, *86*, 2067–2082. [[CrossRef](#)]
9. Chen, S.; Li, P.; Brady, D.; Lehman, B. Determining the optimum grid-connected photovoltaic inverter size. *Sol. Energy* **2013**, *87*, 96–116. [[CrossRef](#)]
10. Perez-Gallardo, J.R.; Azzaro-Pantel, C.; Astier, S.; Domenech, S.; Aguilar-Lasserre, A. Ecodesign of photovoltaic grid-connected systems. *Renew. Energy* **2014**, *64*, 82–97. [[CrossRef](#)]
11. Senol, M.; Abbasoğlu, S.; Kukrer, O.; Babatunde, A. A guide in installing large-scale PV power plant for self consumption mechanism. *Sol. Energy* **2016**, *132*, 518–537. [[CrossRef](#)]
12. Báez-Fernández, H.; Ramirez-Beltran, N.D.; Méndez-Piñero, M.I. Selection and configuration of inverters and modules for a photovoltaic system to minimize costs. *Renew. Sustain. Energy Rev.* **2016**, *58*, 16–22. [[CrossRef](#)]

13. Topić, D.; Knežević, G.; Fekete, K. The mathematical model for finding an optimal PV system configuration for the given installation area providing a maximal lifetime profit. *Sol. Energy* **2017**, *144*, 750–757. [[CrossRef](#)]
14. Durusu, A.; Erduman, A. An improved methodology to design large-scale photovoltaic power plant. *J. Sol. Energy Eng.* **2017**, *140*, 011007. [[CrossRef](#)]
15. Zidane, T.E.K.; Adzman, M.R.; Zali, S.M.; Mekhilef, S.; Durusu, A.; Tajuddin, M.F.N. Cost-effective topology for photovoltaic power plants using optimization design. In Proceedings of the 2019 IEEE 7th Conference on Systems, Process and Control (ICSPC), Malacca, Malaysia, 13–14 December 2019; pp. 210–215.
16. Wang, H.; Muñoz-García, M.; Moreda, G.; Alonso-Garcia, C. Optimum inverter sizing of grid-connected photovoltaic systems based on energetic and economic considerations. *Renew. Energy* **2018**, *118*, 709–717. [[CrossRef](#)]
17. Perez-Gallardo, J.R.; Azzaro-Pantel, C.; Astier, S. Combining multi-objective optimization, principal component analysis and multiple criteria decision making for codesign of photovoltaic grid-connected systems. *Sustain. Energy Technol. Assess.* **2018**, *27*, 94–101. [[CrossRef](#)]
18. Zidane, T.E.K.; Adzman, M.R.; Tajuddin, M.F.N.; Zali, S.M.; Durusu, A. Optimal configuration of photovoltaic power plant using grey wolf optimizer: A comparative analysis considering CdTe and c-Si PV modules. *Sol. Energy* **2019**, *188*, 247–257. [[CrossRef](#)]
19. Bakhshi-Jafarabadi, R.; Sadeh, J.; Soheili, A. Global optimum economic designing of grid-connected photovoltaic systems with multiple inverters using binary linear programming. *Sol. Energy* **2019**, *183*, 842–850. [[CrossRef](#)]
20. Sulaiman, S.I.; Rahman, T.K.A.; Musirin, I.; Shaari, S. Sizing grid-connected photovoltaic system using genetic algorithm. In Proceedings of the 2011 IEEE Symposium on Industrial Electronics and Applications, Langkawi, Malaysia, 25–28 September 2011; pp. 505–509. [[CrossRef](#)]
21. Al-Sabounchi, A.M.; Yalyali, S.A.; Al-Thani, H.A. Design and performance evaluation of a photovoltaic grid-connected system in hot weather conditions. *Renew. Energy* **2013**, *53*, 71–78. [[CrossRef](#)]
22. Kornelakis, A.; Koutroulis, E. Methodology for the design optimisation and the economic analysis of grid-connected photovoltaic systems. *IET Renew. Power Gener.* **2009**, *3*, 476. [[CrossRef](#)]
23. Koutroulis, E.; Yang, Y.; Blaabjerg, F. Co-Design of the PV array and DC/AC inverter for maximizing the energy production in grid-connected applications. *IEEE Trans. Energy Convers.* **2018**, *34*, 509–519. [[CrossRef](#)]
24. Moradi-Shahrbabak, Z.; Tabesh, A.; Yousefi, G.R. Economical design of utility-scale photovoltaic power plants with optimum availability. *IEEE Trans. Ind. Electron.* **2013**, *61*, 3399–3406. [[CrossRef](#)]
25. Okido, S.; Takeda, A. Economic and environmental analysis of photovoltaic energy systems via robust optimization. *Energy Syst.* **2013**, *4*, 239–266. [[CrossRef](#)]
26. Paravalos, C.; Koutroulis, E.; Samoladas, V.; Kerekes, T.; Sera, D.; Teodorescu, R. Optimal design of photovoltaic systems using high time-resolution meteorological data. *IEEE Trans. Ind. Inform.* **2014**, *10*, 2270–2279. [[CrossRef](#)]
27. Ramli, M.; Hiendro, A.; Sedraoui, K.; Twaha, S. Optimal sizing of grid-connected photovoltaic energy system in Saudi Arabia. *Renew. Energy* **2015**, *75*, 489–495. [[CrossRef](#)]
28. Rodrigo, P.M. Improving the profitability of grid-connected photovoltaic systems by sizing optimization. In Proceedings of the 2017 IEEE Mexican Humanitarian Technology Conference (MHTC), Puebla, Mexico, 29–31 March 2017; pp. 1–6.
29. Arefifar, S.A.; Paz, F.; Ordonez, M. Improving solar power PV plants using multivariate design optimization. *IEEE J. Emerg. Sel. Top. Power Electron.* **2017**, *5*, 638–650. [[CrossRef](#)]
30. Camps, X.; Velasco, G.; De La Hoz, J.; Martín, H. Contribution to the PV-to-inverter sizing ratio determination using a custom flexible experimental setup. *Appl. Energy* **2015**, *149*, 35–45. [[CrossRef](#)]
31. Demoulias, C. A new simple analytical method for calculating the optimum inverter size in grid-connected PV plants. *Electr. Power Syst. Res.* **2010**, *80*, 1197–1204. [[CrossRef](#)]
32. Fernández-Infantes, A.; Contreras, J.; Bernal-Agustín, J.L. Design of grid connected PV systems considering electrical, economical and environmental aspects: A practical case. *Renew. Energy* **2006**, *31*, 2042–2062. [[CrossRef](#)]
33. Gemignani, M.; Rostegui, G.; Salles, M.B.C.; Kagan, N. Methodology for the sizing of a solar PV plant: A comparative case. In Proceedings of the 2017 6th International Conference on Clean Electrical Power (ICCEP), Santa Margherita Ligure, Italy, 27–29 June 2017; pp. 7–13.

34. Kerekes, T.; Koutroulis, E.; Sera, D.; Teodorescu, R.; Katsanevakis, M. An optimization method for designing large PV Plants. *IEEE J. Photovoltaics* **2012**, *3*, 814–822. [[CrossRef](#)]
35. Kerekes, T.; Koutroulis, E.; Eyigun, S.; Teodorescu, R.; Katsanevakis, M.; Sera, D. A practical optimization method for designing large PV plants. In Proceedings of the 2011 IEEE International Symposium on Industrial Electronics, Gdansk, Poland, 27–30 June 2011; pp. 2051–2056. [[CrossRef](#)]
36. Kornelakis, A. Multiobjective particle swarm optimization for the optimal design of photovoltaic grid-connected systems. *Sol. Energy* **2010**, *84*, 2022–2033. [[CrossRef](#)]
37. Alsadi, S.; Khatib, T. Photovoltaic power systems optimization research status: A review of criteria, constrains, models, techniques, and software tools. *Appl. Sci.* **2018**, *8*, 1761. [[CrossRef](#)]
38. Baños, R.; Manzano-Agugliaro, F.; Montoya, F.; Gil, C.; Alcayde, A.; Gómez, J. Optimization methods applied to renewable and sustainable energy: A review. *Renew. Sustain. Energy Rev.* **2011**, *15*, 1753–1766. [[CrossRef](#)]
39. Eltawil, M.A.; Zhao, Z. Grid-connected photovoltaic power systems: Technical and potential problems—A review. *Renew. Sustain. Energy Rev.* **2010**, *14*, 112–129. [[CrossRef](#)]
40. Khatib, T.; Mohamed, A.; Sopian, K. A review of photovoltaic systems size optimization techniques. *Renew. Sustain. Energy Rev.* **2013**, *22*, 454–465. [[CrossRef](#)]
41. Mellit, A.; Kalogirou, S.; Hontoria, L.; Shaari, S. Artificial intelligence techniques for sizing photovoltaic systems: A review. *Renew. Sustain. Energy Rev.* **2009**, *13*, 406–419. [[CrossRef](#)]
42. Maatallah, T.; El Alimi, S.; Ben Nassrallah, S. Performance modeling and investigation of fixed, single and dual-axis tracking photovoltaic panel in Monastir city, Tunisia. *Renew. Sustain. Energy Rev.* **2011**, *15*, 4053–4066. [[CrossRef](#)]
43. Singh, N.; Singh, S. A novel hybrid GWO-SCA approach for optimization problems. *Eng. Sci. Technol. Int. J.* **2017**, *20*, 1586–1601. [[CrossRef](#)]
44. Mirjalili, S. SCA: A sine cosine algorithm for solving optimization problems. *Knowl.-Based Syst.* **2016**, *96*, 120–133. [[CrossRef](#)]
45. Energy Information Administration (EIA) USA. Total Electricity Net Generation. 2014. Available online: <https://www.eia.gov/beta/international/data/browser> (accessed on 30 March 2015).
46. Fodhil, F.; Hamidat, A.; Nadjemi, O. Potential, optimization and sensitivity analysis of photovoltaic-diesel-battery hybrid energy system for rural electrification in Algeria. *Energy* **2019**, *169*, 613–624. [[CrossRef](#)]
47. Saiah, S.B.D.; Stambouli, A.B. Prospective analysis for a long-term optimal energy mix planning in Algeria: Towards high electricity generation security in 2062. *Renew. Sustain. Energy Rev.* **2017**, *73*, 26–43. [[CrossRef](#)]
48. Alegria CDER. 2010. Available online: <http://www.cder.dz> (accessed on 12 April 2010).
49. Abada, Z.; Bouharkat, M. Study of management strategy of energy resources in Algeria. *Energy Rep.* **2018**, *4*, 1–7. [[CrossRef](#)]
50. Solar Resource Maps and GIS Data for 200+ Countries. Available online: <https://solargis.com/maps-and-gis-data/download/algerian.d>. (accessed on 7 June 2017).
51. Stambouli, A.B. Promotion of renewable energies in Algeria: Strategies and perspectives. *Renew. Sustain. Energy Rev.* **2011**, *15*, 1169–1181. [[CrossRef](#)]
52. World Bank. World Development Indicators. 2017. Available online: <http://data.worldbank.org/data-catalog/world-development-indicators> (accessed on 1 March 2017).
53. Bouznit, M.; Pablo-Romero, M.D.P. CO₂ emission and economic growth in Algeria. *Energy Policy* **2016**, *96*, 93–104. [[CrossRef](#)]
54. Boukhelkhal, A.; Bengana, I. Cointegration and causality among electricity consumption, economic, climatic and environmental factors: Evidence from North-Africa region. *Energy* **2018**, *163*, 1193–1206. [[CrossRef](#)]
55. Laib, I.; Hamidat, A.; Haddadi, M.; Ramzan, N.; Olabi, A. Study and simulation of the energy performances of a grid-connected PV system supplying a residential house in north of Algeria. *Energy* **2018**, *152*, 445–454. [[CrossRef](#)]
56. Mihoub, S.; Chermiti, A.; Beltagy, H. Methodology of determining the optimum performances of future concentrating solar thermal power plants in Algeria. *Energy* **2017**, *122*, 801–810. [[CrossRef](#)]
57. Ministry of Energy Algeria. Algerian Energy Review N4. May 2015; ISSN 2437-0479. Available online: www.mem-algeria.org (accessed on 15 July 2015).
58. Ministry of Energy Algeria. Objectives New Renewable Energies Program in Algeria (2015-2020-2030). 2015. Available online: www.mem-algeria.org (accessed on 5 September 2015).

59. The Weekend Read: Sustainable Finance—Reassessing Risk, Purpose. Available online: <https://www.pv-magazine.com/2019/08/16/algerian-diesel-solar-tender-concludes-with-lowest-bid-of-11-cents/n.d>. (accessed on 16 August 2019).
60. Fadaee, M.; Radzi, M.A.M. Multi-objective optimization of a stand-alone hybrid renewable energy system by using evolutionary algorithms: A review. *Renew. Sustain. Energy Rev.* **2012**, *16*, 3364–3369. [[CrossRef](#)]
61. Panchula, A.F.; Hayes, W.; Bilash, J.; Kimber, A.; Graham, C. First year performance of a 20 MWac PV power plant. In Proceedings of the 2011 37th IEEE Photovoltaic Specialists Conference, Washington, DC, USA, 19–24 June 2011; p. 001993.
62. Krishnamoorthy, H.S.; Essakiappan, S.; Enjeti, P.N.; Balog, R.; Ahmed, S. A new multilevel converter for Megawatt scale solar photovoltaic utility integration. In Proceedings of the 2012 Twenty-Seventh Annual IEEE Applied Power Electronics Conference and Exposition (APEC), Orlando, FL, USA, 5–9 February 2012; pp. 1431–1438.
63. Marcos, J.; De La Parra, I.; García, M.; Marroyo, L.; Cirés, E. The potential of forecasting in reducing the LCOE in PV plants under ramp-rate restrictions. *Energy* **2019**, *188*, 116053. [[CrossRef](#)]
64. Sharma, V.; Kumar, A.; Sastry, O.S.; Chandel, S. Performance assessment of different solar photovoltaic technologies under similar outdoor conditions. *Energy* **2013**, *58*, 511–518. [[CrossRef](#)]
65. Cabrera-Tobar, A.; Bullich-Massagué, E.; Aragüés-Peñalba, M.; Gomis-Bellmunt, O. Topologies for large scale photovoltaic power plants. *Renew. Sustain. Energy Rev.* **2016**, *59*, 309–319. [[CrossRef](#)]
66. Testa, A.; De Caro, S.; La Torre, R.; Scimone, T. A probabilistic approach to size step-up transformers for grid connected PV plants. *Renew. Energy* **2012**, *48*, 42–51. [[CrossRef](#)]
67. Noorian, A.M.; Moradi, I.; Kamali, G.A. Evaluation of 12 models to estimate hourly diffuse irradiation on inclined surfaces. *Renew. Energy* **2008**, *33*, 1406–1412. [[CrossRef](#)]
68. Demain, C.; Journée, M.; Bertrand, C. Evaluation of different models to estimate the global solar radiation on inclined surfaces. *Renew. Energy* **2013**, *50*, 710–721. [[CrossRef](#)]
69. Liu, B.Y.H.; Jordan, R.C. A rational procedure for predicting the long-term average performance of flat-plate solar-energy collectors with design data for the U. S., its outlying possessions and Canada. *Sol. Energy* **1963**, *7*, 53–74. [[CrossRef](#)]
70. Ayaz, R.; Durusu, A.; Akca, H. Determination of optimum tilt angle for different photovoltaic technologies considering ambient conditions: A case study for Burdur, Turkey. *J. Sol. Energy Eng.* **2017**, *139*, 041001. [[CrossRef](#)]
71. Chin, V.J.; Chin, V.J.; Ishaque, K. Cell modelling and model parameters estimation techniques for photovoltaic simulator application: A review. *Appl. Energy* **2015**, *154*, 500–519. [[CrossRef](#)]
72. Orioli, A.; Di Gangi, A. A procedure to evaluate the seven parameters of the two-diode model for photovoltaic modules. *Renew. Energy* **2019**, *139*, 582–599. [[CrossRef](#)]
73. Elbaset, A.A.; Ali, H.; Sattar, M.A.-E.; Elbaset, A.A. Novel seven-parameter model for photovoltaic modules. *Sol. Energy Mater. Sol. Cells* **2014**, *130*, 442–455. [[CrossRef](#)]
74. Dhoke, A.; Sharma, R.; Saha, T.K. PV module degradation analysis and impact on settings of overcurrent protection devices. *Sol. Energy* **2018**, *160*, 360–367. [[CrossRef](#)]
75. Rosillo, F.G.; Alonso-Garcia, C. Evaluation of color changes in PV modules using reflectance measurements. *Sol. Energy* **2019**, *177*, 531–537. [[CrossRef](#)]
76. Deline, C.; Deline, C. Partially shaded operation of a grid-tied PV system. In Proceedings of the 2009 34th IEEE Photovoltaic Specialists Conference (PVSC), Philadelphia, PA, USA, 7–12 June 2009; pp. 001268–001273. [[CrossRef](#)]
77. Mirjalili, S.; Mirjalili, S.M.; Lewis, A. Grey Wolf Optimizer. *Adv. Eng. Softw.* **2014**, *69*, 46–61. [[CrossRef](#)]

